Geometrical characteristics' impact over the thermal plume modelling with breathing thermal manikins

Ivanov M.[1], Mijorski S.[2]

[1]Senior Assist. Professor, PhD, Technical University of Sofia, FPEPM, Department: "Hydroaerodynamics and Hydraulic Machines", Sofia 1000, Bulgaria

[2]PhD, SoftSim Consult Ltd., Consultant at Technical University of Sofia, FPEPM, Department: "Hydroaerodynamics and Hydraulic Machines", Sofia 1000, Bulgaria

*corresponding author: Martin Ivanov

e-mail: m_ivanov @tu-sofia.bg

Abstract

The presented paper reveals a CFD based analyses of the complexity in the geometrical shape of the thermal manikins, related to their thermal and breathing functions. Both impacts, over velocity and temperature fields in the manikin's thermal plume zone above the head are analyzed for two different geometrical shapes – a physiologically identified (*Humanoid Manikin*) and one designed to match the overall 95th percentile of the anthropometric size of the standard person (*Polygonal Manikin*). The first model represents a comprehensive multifaceted figure of a manikin with high degree of physiological identity with a female human being. The second one is simplified, but still with anatomically realistic component forms, accurately representing the anthropometric size of a standard person. This model, suggested by the authors, allows completely realistic positioning of the hands and legs in the space, and the manikin itself is more convenient for manufacturing of real breathing prototype. The obtained numerical results demonstrate the noticeable impact of the manikins' geometrical characteristics over the simulated breathing and convective flows. The resulting differences have indicted the need of geometrical improvements of the *Polygonal Manikin* in order to match better the real human body thermal plume characteristics.

Keywords: Thermal manikins, CFD modelling, breathing phases

1. Introduction

Nowadays, the virtual and real thermal manikins represent modern, highly complex tools for measurement and analyses of the convective flows around human bodies in different conditions, without excessive risk of exposure to the people themselves. Also, they allow simulating different levels of physical activity, as well as some human actions such as breathing, sweating, sneezing, coughing and others [*Nilsson (2006), Bjørn (1999)*]. Summarized, the thermal manikins are used for global assessment of the human occupants' thermal comfort, as well as for analyses of the indoor air quality in occupied environments. Nevertheless, the experimental studies with real thermal manikins are sometimes expensive and time consuming. Also, they may require highly skilled labor and are relatively difficult to conduct [*Madsen (1999)*]. Therefore, from one side the use of virtual thermal manikins, particularly at the design stage of the indoor environment, seems to be appropriate alternative to the actual thermal manikins' experiments [*Ivanov (2015)*]. But on the other side, the need of relatively inexpensive and easy to construct and use real thermal manikins will always exists, considering that all performed simulation studies need to be verified and validated with experimental measurement data. Such simplified structure of a virtual thermal manikin with breathing function is suggested by the authors in the current paper, and the first stage of the breathing flow modeling is presented in *Ivanov and Mijorski (2017)*. But still, implementation of CFD based intelligent technologies is required, in order to assess the design performance of the developed virtual breathing thermal manikin. That is why the objective of the presented study is to analyze the geometrical characteristics' impact over the thermal plume modelling with breathing thermal manikins. The main task is to develop and perform simulation studies of the breathing cycle flow for the both manikin geometries – the physiologically identical one (called *Humanoid Manikin*) and the proposed simplified shape one (called *Polygonal Manikin*). The differences or the similarities in the velocity and thermal flow fields between the two shapes will provide initial assessment measure for the both models performance.

2. 3D geometry modelling of the manikins

The multifaceted 3D female manikin was remodeled and adapted for the purpose of the study. It represents with high degree of physiological identity a real female human being, and has an approximate surface area of 1.8 m^2 and height of 1.65 m. The nasal valve opening was constructed according to the study of *Lin (2015)* and was initially used by the authors in *Ivanov and Mijorski (2017)*. As shown in Fig.1, the opening nasal area is 7.3 x 10^{-5} m^2. The normal to the nasal opening was specified to 45 degrees from the vertical body axis. Additionally, exhaust walls from the nasal valve to the nose end were inclined to 15 degrees according to *Nilsson (2006) and Lin (2015)*. The developed *Polygonal Manikin* (with an approximate surface area of 2.0 m^2 and height of 1.75 m) represents an appropriate form, structure and design, which meet the basic

requirements of the ergonomic design area. It is designed by Georgi Chervendinev (*Engineering Design Lab at TU-Sofia*) for use in real research applications, as well as for educational purposes. The virtual manikin is developed using parametric design software, which allows easy modifications and comply with the following requirements:

• Manufacturability. Seeking for a solution that would be easily feasible, with different materials without requiring the use of expensive tooling. The form consists of planar elements that make a polygonal structure. The manikin could be manufactured by various sheet materials like sheet metal, plywood and others. It may also be made with additive technologies, like 3D printing.

• Mobility. Construction of the moving parts, that allows optimal simulation of the human movements, for the needs of ergonomic research. The individual elements are connected by cylindrical or spherical joints.

• Availability in different scales. Proposed are variants with different numbers of polygons and joints, allowing to be selected a case-optimal scale. At a larger scale (smaller dimensions), the manikin can be manufactured without joints and a reduced number of polygons. In this case, a variety of operating positions can also be performed, and the same could be done in the virtual manikin model.

• Ability to perform different motion degrees. In the cases where the movement of human hands and legs are not the subject of study, it is possible to manufacture the manikin with a smaller number of movable joints or without any. Then the internal body volume is maximized, allowing the installation of different devices, simulating human activities, such as breathing, coughing, sneezing and so on.

• Open design. The polygonal shape, constructed from planar elements, allows easy addition of extra elements. It is also possible to easily install various sensors and auxiliary devices over the planar surface.

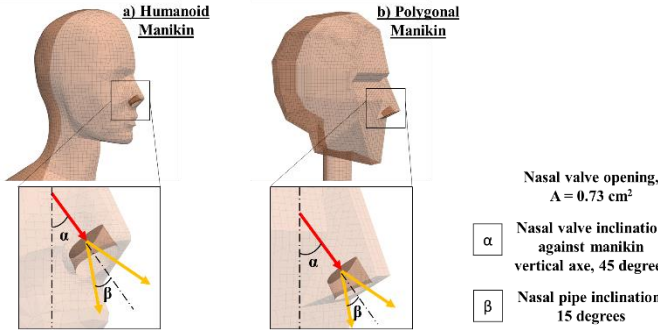

Figure 1. 3D models and nasal valve geometry details

3. Spatial discretization and model setup

3.1. Spatial discretization

The two 3D models of the thermal manikin in the context of rectangular shaped room were discretized with *snappyHexMesh* utility, part of an ENGYS® (*www.engys.com*) enhanced version of the CFD code OpenFoam® (*www.openfoam.com*). The generated numerical grids were with total of 1 140 000 poly-mesh control volume elements for the *Humanoid Manikin* and 1 417 722 poly-mesh cells for the *Polygonal Manikin*. The base cell size was defined to 4 10^{-2} m, for both models. In order to capture the nasal valve geometrical features the maximum level of cells refinement reached 6.25 10^{-4} m. The current meshes are well refined at the surfaces of the manikins, with a first layer height of approximately 0.5 10^{-3} m. The levels of refinement were assessed with a detailed analysis of the y+ values over the manikin surfaces. In the specified exhale air flow conditions the y+ values were below 4 to all surface cells of the models (see Fig. 2) as recommended in the work of *Spalart (2001)*. Thus, the models matched the requirements for resolving accurately the turbulent flow over manikins' surfaces in the set of RANS (*Reynolds-Averaged Navier-Stokes*) CFD simulations.

3.2. Solver and turbulence model

Two sets of 3D steady state simulations, based on RANS equation method were performed. All three phases of the human breathing cycle were modeled for each of the manikin models, including: inhaling, exhaling and no breathing (the free convection flow case). The solver for the buoyant turbulent flow of incompressible fluids *buoyantBoussinesqSimpleFoam* with combinations of semi-implicit method for pressure-linked equations (SIMPLE) algorithms was employed for all simulations. Additionally, the Shear Stress Transport (SST) k-ω turbulence model was applied in the simulations, as suggested in *Menter (1993)*. This is a two-equation eddy-viscosity model, where the SST model formulation combines the use of a k-ω in the inner parts of the boundary layer, but also switches to a k-ε behavior in the free-stream regions of the computational domain. Further details of the selected RANS turbulence model can be found in work of *Menter (2011)*. The resolving of the buoyant flow close to the manikins' surface is associated with high nonlinearity of the solutions and there could be small fluctuations in the velocity and pressure fields even under steady state conditions, especially in the more refined zones. To compensate this, a flow averaging at the final 1000 iterations was introduced for each simulation. This helped in the smoothing of any small flow fluctuations in the most refined zones of the domains.

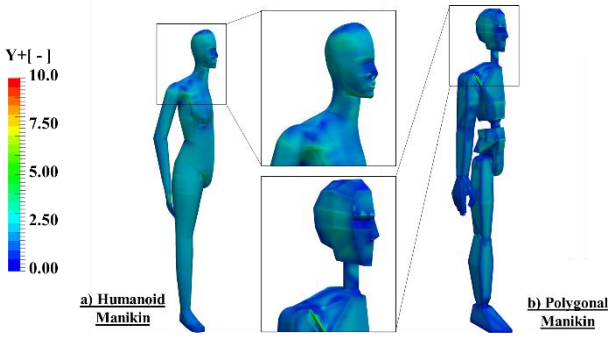

Figure 2. Y+ fields over manikins' surface

Table 1. Implemented boundary conditions

Boundary Name	Boundary Conditions	Inhale	Free convection flow	Exhale
No Slip Walls	Surface temperature, 20 [^{o}C]	Yes	Yes	Yes
Vent Opening	Air temperature and pressure, 20 [^{o}C] and 101325 [Pa]	Yes	Yes	Yes
Manikin	Fixed heat flux as per Fig.3	Yes	Yes	Yes
Nose inlet	Inlet flow rate, 6.29 10^{-4} [m^3/s] at 36 [^{o}C]	No	No	Yes
Nose outlet	Outlet flow rate, 6.91 10^{-4} [m^3/s]	Yes	No	No
Symmetry	Symmetry plane	Yes	Yes	Yes

3.3. Initial and Boundary conditions

The material properties of the modeled fluid were modified as well, in order to match the reference conditions where the pressure was 101325 Pa and air temperature was 20 ^{o}C. Thus the air density was 1.204kg/m^3; dynamic viscosity was 1.82 10^{-5} kg/(m.s); kinematic viscosity was 1.51 10^{-5} m^2/s and specific heat was 1006.0 J/(kg·K). In Table 1 and Fig.3 are given all the different boundary conditions adopted in the CFD simulations, together with the associated heat fluxes from the thermal manikins. The heat fluxes were derived from the study of *Nilsson (2006)*, based on total heat release rate of 110 W for the whole manikin surface. The nasal valve openings were specified as velocity inlet for exhale phase and outlet for the inhale. The flow rates were calculated based on the study of *Lin (2015)*. The total flow rates for both inhaling and exhaling were approximated as follows:

$$Q = (\Delta P.\pi.r^4) / (8.\eta.L) \quad (1)$$

Where:

- Q, total flow rate during inhaling and exhaling, m^3/s;
- ΔP, pressure in the range of 40-80 Pa, selected value of 60 Pa;
- L, approximated nasal valve length, 0.33 m;
- r, approximated nasal valve radius, 0.11 m;
- η, kinematic viscosity, m^2/s;
- η_{20}, η at 20 ^{o}C, 1.51 10^{-5} m^2/s;
- η_{36}, η at 36 ^{o}C, 1.66 10^{-5} m^2/s.

The Reynolds number for the nasal flow was approximated based on the eq. 2.

$$Re = 2.r.Q.\rho/\eta \quad (2)$$

This way the turbulent intensity for the velocity inlet was calculated to 6.8 %.

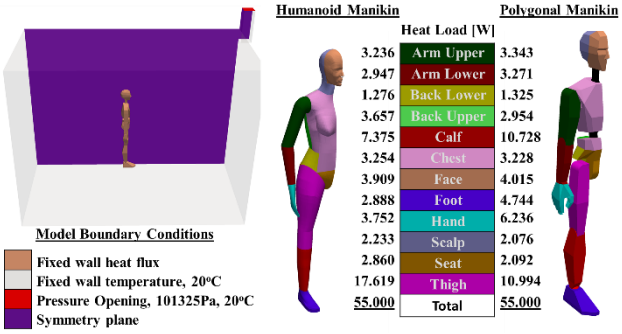

Figure 3. CFD model boundary conditions

4. Numerical results and discussion

The numerical results are presented in from of velocity and temperature fields for the exhale phase of the flow. Two different sections from the solutions are extracted. The first is a perpendicular section to the symmetry plane of the domain and the second is at the symmetry plane. Additionally, it is presented a pointwise data in graphical format, at a horizontal profile above the manikins' head and parallel to the symmetry plane at 2.5 m height from the floor. There are visible differences in the velocity and temperature fields in both sections from the solutions. The resulted thermal plume in the case of *Polygonal Manikin* is with lower velocity and temperature and it is more diffused above the head with wider shape of the flow (see Fig.4 and Fig.5). The maximum velocity measured in the *Humanoid* free convection flow model was 0.6 m/s, while in the *Polygonal* this value dropped to 0.54 m/s.

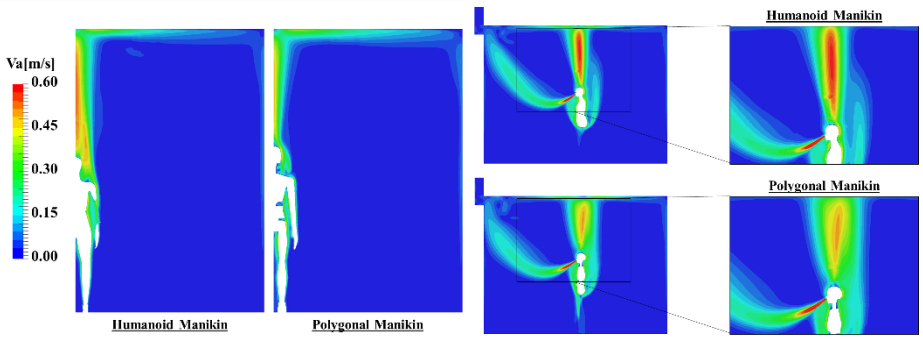

Figure 4. Velocity fields - exhale breathing phase

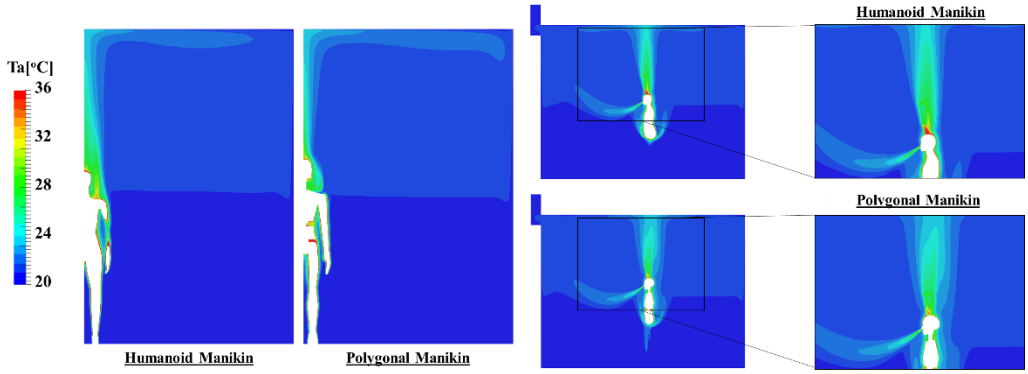

Figure 5. Temperature fields - exhale breathing phase

.

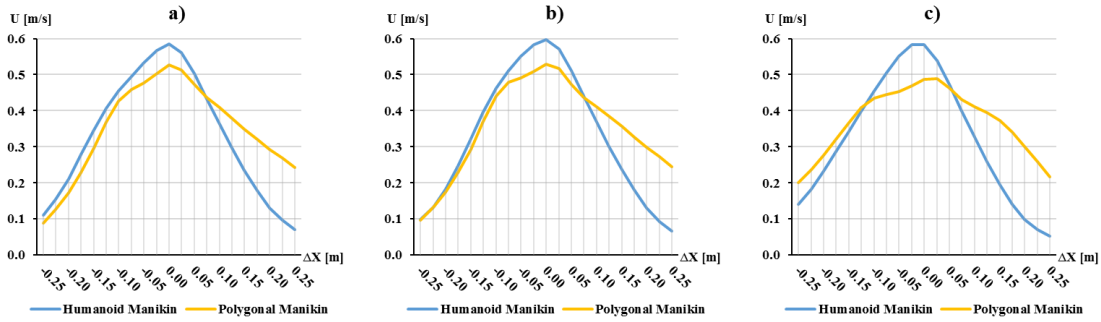

Figure 6. Horizontal air velocity at monitoring points: a) Inhale; b) Free convection; c) Exhale

The observation regarding the shape of the plume can be confirmed also from the horizontal graphical data in Fig.6, where the profile of *Humanoid Manikin* is with more distinguished peak at the center, while in the polygonal model is more outspread with smoother gradients at the end from the back side of the manikin. The increased separations of the free convective flow along the *Polygonal Manikin* are the main driving force for the noticeable differences in the illustrated comparative plots. The polygonal structures of the *Polygonal Manikin* have resulted in sharp edges at all body parts. Together with the mobility feature, which required recess zones and many additional openings, it leads to recirculation zones and stronger flow separations compared to the *Humanoid Manikin* model. The effect of such zones is more strongly observed at the recess below the head and at the big gap between upper and lower backs for the *Polygonal Manikin***5.**

5. Conclusions

The comparative analysis of the numerical results has illustrated several weaknesses of the proposed *Polygonal Manikin* model. Sharp edges and big recess zones significantly alters the free convection flow compared to the *Humanoid Manikin*. The recirculation zones and increased flow separation leaded to wider thermal plume above the head of the manikin with lower air velocity and temperature. Introduction of model modifications, in order to mitigate the observed issues, is advisable for improvement of the manikin performance. Such modifications would be the installation of flexible collars and additional post-manufacturing filleting of the sharp edges. However, before taking final decisions regarding the improvements of the *Polygonal Manikin*, it will be beneficial if additional numerical analyses are performed, investigating the impact of the proposed mitigation measures.

Acknowledgements

The presented study is supported by “RDS” at TU-Sofia, as part of the activities under the "Perspective leaders" project, with Contract № 171ПР0016-02, entitled: “Implementation of CFD based intelligent technologies, for design assessment of developed virtual breathing thermal manikin".

References

Bjørn E., (1999), „Simulation of human respiration with breathing thermal manikins“, Proceedings of the 3rd international meeting on thermal manikin testing 3IMM, Stockholm, Sweden, 12–13 October;

Ivanov M., (2015), “Compact Breathing Simulation System, Developed as Additional Functionality for Thermal Manikins”, “Romanian Journal of Building Services”, Vol.1, No.3, ISSN: 2393-5154, pp. 1-12;

Ivanov M., Mijorski S., (2017), “CFD modelling of flow interaction in the breathing zone of a virtual thermal manikin”, “Energy Procedia” Journal, Volume 112, pp. 240-251, ISSN: 1876-6102, Elsevier;

Lin S., (2015), “Nasal Aerodynamics”, Chief Editor: Arlen D Meyers, MD, MBA, http: //emedicine. medscape.com/article/874822-overview#a1, Updated: May 14, 2015;

Madsen T., (1999), “Development of a breathing thermal manikin”, Proceedings of the 3rd international meeting on thermal manikin testing 3IMM, Stockholm, Sweden, 12–13 October;

Menter F., (1993), "Zonal Two Equation k-ω Turbulence Models for Aerodynamic Flows", AIAA Paper 93-2906;

Menter F., (2011), “Turbulence Modelling for Engineering Flows”, ANSYS Inc.;

Nilsson H., (2006) “How to Build and Use a Virtual Thermal Manikin Based on Real Manikin Methods”, Sixth International Thermal Manikin and Modelling Meeting”, “Thermal Manikins and Modelling”, ISBN: 962-367-534-8;

Spalart P., (2001), Young-person’s guide to detached-eddy simulations grids, NASA/CR-2001-21103, Boeing Commercial Airplanes, Seattle, Washington.